Mon. Not. R. Astron. Soc. **338,** 389–400 (2003)

Non-radial oscillation modes as a probe of density discontinuities in neutron stars

G. Miniutti,[1] J. A. Pons,[1] E. Berti,[2] L. Gualtieri[1] and V. Ferrari[1]⋆

[1]*Dipartimento di Fisica 'G. Marconi', Università di Roma 'La Sapienza' and Sezione INFN ROMA1, piazzale Aldo Moro 2, I-00185 Roma, Italy*
[2]*Department of Physics, Aristotle University of Thessaloniki, Thessaloniki 54006, Greece*

Accepted 2002 September 10. Received 2002 September 9; in original form 2002 June 11

ABSTRACT

A phase transition occurring in the inner core of a neutron star could be associated with a density discontinuity that would affect the frequency spectrum of the non-radial oscillation modes in two ways. First, it would produce a softening of the equation of state, leading to more compact equilibrium configurations and changing the frequency of the fundamental and pressure modes of the neutron star. Secondly, a new non-zero frequency g mode would appear, associated with each discontinuity. These discontinuity g modes have typical frequencies larger than those of g modes previously studied in the literature (thermal, core g modes or g modes caused by chemical inhomogeneities in the outer layers), and smaller than that of the fundamental mode; therefore they should be distinguishable from the other modes of non-radial oscillation. In this paper we investigate how high-density discontinuities change the frequency spectrum of the non-radial oscillations, within the framework of the general relativistic theory of stellar perturbations. Our purpose is to understand whether a gravitational signal, emitted at the frequencies of the quasi-normal modes, may give some clear information on the equation of state of the neutron star and, in particular, on the parameters that characterize the density discontinuity. We discuss some astrophysical processes that may be associated with the excitation of these modes, and estimate how much gravitational energy should the modes convey to produce a signal detectable by high-frequency gravitational detectors.

Key words: gravitational waves – relativity – stars: neutron – stars: oscillations.

1 INTRODUCTION

The equation of state (EOS) of dense matter at supranuclear densities has been a long sought-after problem in nuclear physics. Since the first observational evidence of their existence in the late 1960s, neutron stars (NS) have proved to be a unique astrophysical environment in which very different fields of physics, ranging from nuclear physics to particle physics and general relativity, can be tested. Accurate estimates of some properties of NSs, such as masses and radii, associated with further information on the thermal history, would allow one to set constraints on the nature of nuclear forces. This has been attempted by several means (but so far with limited success), by correlating multiwavelength observations with different telescopes, X-ray or γ-ray observatories (Thorsett & Chakrabarty 1999; Rutledge et al. 2001; Pons et al. 2002b), or through the study of neutrinos from protoneutron stars (Pons et al. 1999, 2001) or studying quasi-periodic object properties (Osherovich & Titarchuk 1999; Stella & Vietri 1999).

In the near future, a new observational window will be opened by a network of gravitational wave detectors: the ground-based interferometers (LIGO, VIRGO, GEO600, TAMA), which are now in the final stage of construction or in the commissioning phase, will explore the frequency region of 10–1000 Hz, and the space-based interferometer *LISA* will enlarge the observational window to 10^{-4}–10^{-1} Hz. In addition, a joint panel of European experts have performed an assessment study for a new generation of interferometric detectors with extremely high sensitivity in the kHz region (EURO, EURO–XYLOPHONE), which would provide a very powerful means to investigate the physics of neutron stars through gravitational waves. Since these instruments are currently under study, it is important to envisage which sources they would be able to see, and what kind of information could be inferred from the detected signals. In this paper, we address one interesting possibility in this exciting new field: the prospect of probing phase transitions occurring in the inner core of neutron stars. In particular, we shall focus on phase transitions that produce a density discontinuity.

⋆E-mail: valeria@roma1.infn.it

Density discontinuities may occur either at high or low density, depending on the physical processes prevailing in the different regions of the star. At low density, the characteristic chemical profile in the outer layers is determined by the history of the star, because shell burning, flash nuclear burning and accretion phenomena leave layers of different composition on its surface. At the interfaces between different layers, the chemical composition changes abruptly, and if no significant diffusion is present, the density gradient is well approximated by a discontinuity. This introduces an additional local source of buoyancy that gives rise to a discontinuity g mode, even if no other source of buoyancy is present, i.e. even in zero-temperature NSs. The properties of the g modes owing to discontinuities in the outer layers in cold NSs have been studied by Finn (1987) and McDermott (1990). Subsequently, Strohmayer (1993) computed the oscillation frequencies of two finite-temperature models with a density discontinuity associated to the ^{56}Fe–^{62}Ni transition. He found that if the discontinuity is trapped into the crust no mode can be found directly associated with it, while if it is located in the fluid ocean a g mode appears, and the frequency distribution of the g modes owing to entropy gradients changes.

However, density discontinuities are not necessarily confined to the outer layers of a neutron star: they could also arise as a consequence of phase transitions in the inner core, where the equation of state is still poorly known. Several first- or second-order phase transitions have been proposed to occur at supranuclear densities, and they typically involve pion and/or kaon condensation and the transition from ordinary nuclear matter to quark matter (Heiselberg & Hjorth-Jensen 2000; Prakash et al. 1997 and references therein). Whether these transitions are first or second order, and whether they admit density discontinuities or a continuous transition with a mixed phase, is still a matter of debate. In modelling the phase transition, one possibility is to impose local conservation laws and to use a Maxwell construction, which produces a density discontinuity. Glendenning (1992) pointed out that, since conservation laws must be imposed globally, any first-order phase transition should be accompanied by a smooth mixed phase region, which satisfies the Gibbs rules. However, it should be noted that there is much uncertainty on the effect that Coulomb repulsive forces and surface tension have on the structure of the mixed phase. If Coulomb and surface energies are large, the mixed phase is disfavoured, the region where it occurs shrinks, and this seems to be the case in a quark–hadron phase transition (Alford et al. 2001). In this case, density discontinuities may appear near the boundaries of the Gibbs structured phase, when the volume fraction of one of the phases is very small.

Astrophysical observations play an important role in clarifying these issues, because neutron stars provide a unique opportunity to study the behaviour of matter in this very high-density regime. In the present paper we study how density discontinuities affect the spectrum of the quasi-normal modes of a neutron star, with the purpose of understanding what kind of information can be inferred on the high-density equation of state from the gravitational signal emitted by an oscillating neutron star. We shall consider some astrophysical processes in which the quasi-normal modes could be excited (a glitch, the onset of the phase transition, binary coalescence of NSs) and we shall estimate the amount of energy that should go into such modes to produce a signal that may be detected by the proposed high-frequency gravitational detectors. In this respect, our work differs from the previous work of Sotani, Tominaga & Maeda (2001), who focused on the calculation of the modes and discussed the stability of the considered models. For simplicity, we consider the case of cold neutron stars and assume a simple polytropic EOS.

In Section 2 we briefly describe the relevant equations of stellar perturbations that we integrate to find the mode frequencies. In Section 3 we discuss the results of the integration, extracting the information that the discontinuity g modes carry on the parameters of the density discontinuity. In Section 4 we consider some astrophysical processes that are associated with the excitation of the quasi-normal modes, and discuss the detectability of the emitted gravitational radiation. In Section 5 we draw our conclusions.

2 THE MATHEMATICAL FRAMEWORK

In order to find the frequencies of the quasi-normal modes, we will integrate the equations describing the polar, non-radial perturbations of a non-rotating star as formulated by Lindblom & Detweiler (1983) and Detweiler & Lindblom (1985). We write the perturbed metric tensor as

$$\mathrm{d}s^2 = -\mathrm{e}^{\nu}\left(1 + r^l H_{0lm} Y_{lm} \mathrm{e}^{\mathrm{i}\omega t}\right)\mathrm{d}t^2 - 2i\omega r^{l+1} H_{1lm} Y_{lm} \mathrm{e}^{\mathrm{i}\omega t}\,\mathrm{d}t\,\mathrm{d}r + \mathrm{e}^{\lambda}\left(1 - r^l H_{0lm} Y_{lm} \mathrm{e}^{\mathrm{i}\omega t}\right)\mathrm{d}r^2 + r^2\left(1 - r^l K_{lm} Y_{lm} \mathrm{e}^{\mathrm{i}\omega t}\right)\left(\mathrm{d}\theta^2 + \sin^2\theta\,\mathrm{d}\phi^2\right), \tag{1}$$

and the polar components of the Lagrangian displacement of the perturbed fluid elements as

$$\begin{aligned} \xi^r &= \mathrm{e}^{-\lambda/2} r^{l-1} W_{lm} Y_{lm} \mathrm{e}^{\mathrm{i}\omega t}, \\ \xi^\theta &= -r^{l-2} V_{lm} \partial_\theta Y_{lm} \mathrm{e}^{\mathrm{i}\omega t}, \\ \xi^\phi &= -r^l (r\sin\theta)^{-2} V_{lm} \partial_\phi Y_{lm} \mathrm{e}^{\mathrm{i}\omega t}, \end{aligned} \tag{2}$$

where $Y_{lm}(\theta, \phi)$ are the spherical harmonic functions. In the following we shall restrict our analysis to the $l = 2$ component, which dominates the emission of gravitational radiation. By defining the variable X,

$$X = \omega^2(\rho + p)\mathrm{e}^{-\nu/2} V - r^{-1}\mathrm{e}^{(\nu-\lambda)/2} p' W + \frac{1}{2}(\rho + p)\mathrm{e}^{\nu/2} H_0, \tag{3}$$

where p and ρ are the pressure and energy density of the fluid and the prime indicates differentiation with respect to r, one can write a fourth-order system of linear equations for (H_1, K, W, X),

$$
\begin{aligned}
H_1' &= \frac{1}{r}\left(-\{(l+1)+\mathrm{e}^{\lambda}[2M(r)/r+r^2(p-\rho)]\}H_1+\mathrm{e}^{\lambda}[H_0+K-4(\rho+p)V]\right),\\
K' &= \frac{1}{r}\left\{H_0+(n+1)H_1-\left[(l+1)-r\frac{1}{2}\nu'\right]K-2(\rho+p)\mathrm{e}^{\lambda/2}W\right\},\\
W' &= -\frac{(l+1)}{r}W+r\mathrm{e}^{\lambda/2}\left[\frac{\mathrm{e}^{-\nu/2}X}{\gamma p}-\frac{l(l+1)V}{r^2}+\frac{1}{2}H_0+K\right],\\
X' &= -\frac{l}{r}X+(\rho+p)\mathrm{e}^{\nu/2}\left(\frac{1}{2}\left(\frac{1}{r}-\frac{1}{2}\nu'\right)H_0+\frac{1}{2r}[r^2\tilde{\omega}^2+(n+1)]H_1+\frac{1}{2r}\left(\frac{3}{2}r\nu'-1\right)K\right.\\
&\quad\left.-\nu'\frac{l(l+1)V}{2r^2}-\frac{1}{r}\left\{\mathrm{e}^{\lambda/2}[(\rho+p)+\tilde{\omega}^2]-\frac{1}{2}r^2(r^{-2}\mathrm{e}^{-\lambda/2}\nu')'\right\}W\right),
\end{aligned}
\tag{4}
$$

where $n=(l-1)(l+2)/2$, $\tilde{\omega}^2=\omega^2\mathrm{e}^{-\nu}$ and γ is the adiabatic index,

$$
\gamma=\frac{\rho+p}{p}\left(\frac{\partial p}{\partial\rho}\right)_{\mathrm{s}}=\frac{\rho+p}{p}c_{\mathrm{s}}^2. \tag{5}
$$

The functions V and H_0 are

$$
\begin{aligned}
H_0 &= \frac{2r^2\mathrm{e}^{-\nu/2}X-\left[\frac{1}{2}(n+1)r\nu'-r^2\tilde{\omega}^2\right]\mathrm{e}^{-\lambda}H_1+\left\{n-\tilde{\omega}^2r^2-\frac{1}{2}\nu'[3M(r)-r+r^3p]\right\}K}{3M(r)/r+n+r^2p}\\
V &= \frac{1}{\tilde{\omega}^2}\left[\frac{X\mathrm{e}^{-\nu/2}}{(\rho+p)}-\frac{\nu'\mathrm{e}^{-\lambda/2}W}{2r}-\frac{1}{2}H_0\right].
\end{aligned}
\tag{6}
$$

For each given value of l and ω, equation (4) admits only two linearly independent solutions regular at $r=0$; we find the general solution as a linear combination of the two, such that the perturbation of the Lagrangian pressure, Δp, vanishes at the surface. This procedure is slightly different from that proposed by Lindblom & Detweiler (1983), but a comparison of the results of the two procedures shows that they are absolutely equivalent.

It should be noted that, in this formulation, both ξ^r and Δp are continuous even when the density is discontinuous.

It is well known that outside the star, the variables associated with the fluid motion are zero and the equations reduce to a second-order equation for the Zerilli function Z,

$$
\left(\frac{\mathrm{d}^2}{\mathrm{d}r_*^2}+\omega^2\right)Z=UZ,\quad U=\frac{2(r-2M)}{r^4(nr+3M)^2}\left[n^2(n+1)r^3+3Mn^2r^2+9M^2(M+nr)\right], \tag{7}
$$

where $r_*\equiv r+2M\log(r/2M-1)$ and M is the mass of the star. The asymptotic behaviour of the Zerilli function is

$$
Z\sim A_{\mathrm{in}}(\omega)\mathrm{e}^{-\mathrm{i}\omega r_*}+A_{\mathrm{out}}(\omega)\mathrm{e}^{\mathrm{i}\omega r_*}. \tag{8}
$$

A quasi-normal mode of the star is defined to be a solution of the perturbed equations belonging to a complex eigenfrequency $\omega_0+\mathrm{i}\,\omega_{\mathrm{im}}$, which is regular at the centre, continuous at the surface and which behaves as a pure outgoing wave at infinity. Therefore, if ω_0 is the mode frequency, $A_{\mathrm{in}}(\omega_0)$ must vanish. In order to find the frequency of the quasi-normal modes we use the following algorithm (Chandrashekar & Ferrari 1990), which is appropriate when the real part of the frequency ω_0 is much larger than the imaginary part $\omega_{\mathrm{im}}=1/\tau$, as it is in our case. For real values of the frequency, the function Z must have the asymptotic form

$$
\begin{aligned}
Z\to &\left\{\alpha-\frac{n+1}{\omega}\frac{\beta}{r}-\frac{1}{2\omega^2}\left[n(n+1)\alpha-3M\omega\left(1+\frac{2}{n}\right)\beta\right]\frac{1}{r^2}+\cdots\right\}\cos\omega r_*\\
&-\left\{\beta+\frac{n+1}{\omega}\frac{\alpha}{r}-\frac{1}{2\omega^2}\left[n(n+1)\beta+3M\omega\left(1+\frac{2}{n}\right)\alpha\right]\frac{1}{r^2}+\cdots\right\}\sin\omega r_*.
\end{aligned}
\tag{9}
$$

The functions $\alpha(\omega)$ and $\beta(\omega)$ can be determined by matching the numerically integrated solution with the above asymptotic expression for Z. The amplitude of the standing gravitational wave at infinity is $(\alpha^2+\beta^2)^{1/2}$ and it can be shown to have a deep minimum at the frequency ω_0 where $A_{\mathrm{in}}(\omega_0)$ vanishes (Chandrasekhar, Ferrari & Winston 1991); thus, we find the frequency of a quasi-normal mode by searching for the values of ω_0 where $(\alpha^2+\beta^2)^{1/2}$ has a minimum.

3 RESULTS

To study the effect of high-density discontinuities on the oscillation spectrum of a NS, we shall consider a simple polytropic equation of state of the form

$$
p=\begin{cases}K\rho^{\Gamma} & \rho>\rho_{\mathrm{d}}+\Delta\rho\\ K\left(1+\dfrac{\Delta\rho}{\rho_{\mathrm{d}}}\right)^{\Gamma}\rho^{\Gamma} & \rho<\rho_{\mathrm{d}},\end{cases} \tag{10}
$$

where the discontinuity of amplitude $\Delta\rho$, is located at a density $\rho_{\rm d}$, which we choose to be greater than the nuclear saturation density $\rho_0 = 2.8 \times 10^{14}$ g cm^{-3}. This simplified equation of state will allow us to study in a systematic way the properties of the quasi-normal modes, and the relation between the mode frequencies and the global properties of the chosen models. This EOS has been used in the past to study the g modes associated with low-density discontinuities (Finn 1987; McDermott 1990) and, in a slightly modified form, to study the g modes caused by high-density discontinuities (Sotani et al. 2001).

To find the frequency of the surface g modes, Finn introduced the so-called slow-motion formalism (Finn 1986), which is very accurate in the low-frequency limit. In our case the mode frequencies are higher since they are associated with high-density discontinuities, and the full system of perturbation equations has to be integrated. As a consistency check of our code, we have repeated some of Finn's calculations for low-density discontinuities (Finn 1987) finding an excellent agreement (better than three significant digits).

It should be mentioned that g modes may have a real, imaginary or zero frequency, depending on whether the considered stellar model is stable under convection; different regimes can be identified by looking at the sign of the square of the Brunt-Väisälä frequency

$$N^2 = \frac{1}{2} e^{\nu-\lambda}\, \nu' \frac{p'}{p}\left(\frac{1}{\gamma} - \frac{1}{\gamma_0}\right), \quad \text{with} \quad \gamma_0 = \frac{\rho + p}{p}\frac{p'}{\rho'}. \tag{11}$$

A real, imaginary or zero N correspond, respectively, to convective stability, instability or marginal instability. If the star is isentropic and chemically homogeneous, $\gamma = \gamma_0$ and all g modes degenerate to zero frequency. Thus, in the case of our zero-temperature, chemically homogeneous star, N is zero everywhere, except when the density changes abruptly at $r = R_{\rm d}$; at that point, the adiabatic index γ remains finite, the equilibrium index γ_0 vanishes, N is different from zero and a g mode appears.

Before discussing the behaviour of the quasi-normal mode frequencies, let us briefly describe how the structure of a neutron star changes if a phase transition associated with a density discontinuity occurs in its inner core. In Fig. 1 we plot the mass–radius relation for a star with and without discontinuity. In both cases the polytropic index is $\Gamma = 2$. In order to compare stars that have the same equation of state for $\rho < \rho_{\rm d}$, we set $K = 180$ km^2 for the star without discontinuity, and $K(1 + \Delta\rho/\rho_{\rm d})^2 = 180$ km^2 for one with a discontinuity (we choose $\rho_{\rm d} = 7 \times 10^{14}$ g cm^{-3} and $\Delta\rho/\rho_{\rm d} = 0.3$). In this way we also ensure that the compressibility of the matter in the low-density region is the same. Fig. 1 shows that the maximum mass is lower for the model with a density discontinuity; this is a general behaviour, which is caused by the softening of the equation of state introduced by the discontinuity. As a rule of thumb, for a fixed mass, a star with a discontinuity is more compact than one with the same mass and no discontinuity at all; for instance, from Fig. 1 we see that for $M = 1.4\ {\rm M}_\odot$ the star with no phase transition has a radius of $R = 13.44$ km, while one with a density discontinuity has $R = 9.66$ km. These general properties continue to also hold if EOSs more realistic than equation (10) are used, and if phase transitions arising from kaon/pion condensation or from the nucleation of quark matter are considered (Heiselberg & Hjorth-Jensen 2000). Thus the EOS we use, though approximate, allows us to infer the mode properties that are known to depend much more on the macroscopic properties of the star (mass, radius, etc.), than on the specific microscopic interactions.

In our study, we shall consider stars with a fixed mass $M = 1.4\ {\rm M}_\odot$ because astronomical observations show that NSs that have not spent a significant part of their life accreting matter from a companion in a binary system, have masses in a narrow range around this fiducial value (Thorsett & Chakrabarty 1999). We shall choose different values of the polytropic exponent $\Gamma = (1.67, 1.83, 2.00, 2.25)$, and assign the constant K in such a way that models with the same Γ have the same EOS for $\rho < \rho_{\rm d}$, independent of the particular values of $\Delta\rho/\rho_{\rm d}$ and $\rho_{\rm d}$. Since we require that all stars have the same mass, we will have to adjust the central density accordingly. This means that different stars have a different matter content in their core. Furthermore, we select models with reasonable radii ($8.5 \leqslant R \leqslant 17.9$ km) and, since we want to

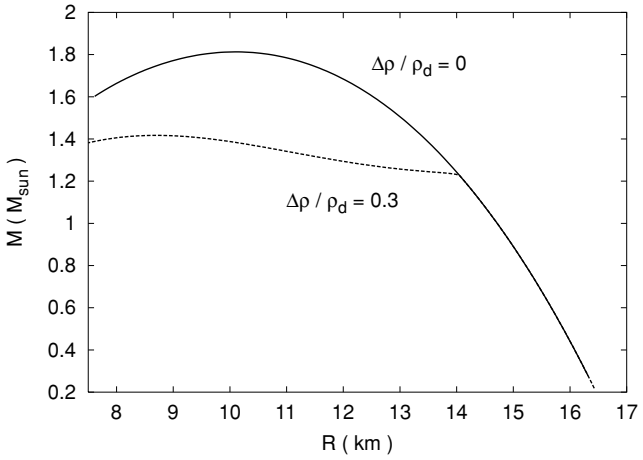

Figure 1. We compare the mass–radius curve of stellar models without a discontinuity (continuous line) and with a high-density discontinuity in the core (dashed line). Both curves refer to the same low-density equation of state with $\Gamma = 2$, the only difference being the presence of a discontinuity at $\rho_{\rm d} = 7 \times 10^{14}$ g cm^{-3} with $\Delta\rho\ /\rho_{\rm d} = 0.3$, for the model shown with a dashed line. As discussed in the text, when a discontinuity is present the star is more compact and the maximum mass is lower.

study high-density discontinuities, we fix their location at $R_d \leqslant 0.8R$. The amplitude of the discontinuity is chosen to vary within $\Delta\rho/\rho_d =$ (0.1–0.3); larger values would not allow stable stellar models with reasonable values of mass and radius.

In Tables 1–4 we summarize the results of the numerical integration of equations (4) and (7) for these stellar models, and the equilibrium parameters. The frequencies of the fundamental mode (ν_f), the first pressure mode (ν_p) and the discontinuity g mode (ν_g) are tabulated for different values of the parameters. The models considered in Table 1 have the same value of the polytropic exponent, $\Gamma = 2$, and refer to three

Table 1. The frequencies of the fundamental mode, of the first p mode and of the discontinuity g mode are shown for a set of stellar models with $M = 1.4\,M_\odot$ and $\Gamma = 2$. For each star, the equilibrium parameters are also tabulated. The polytropic coefficient K is $K\,(1 + \Delta\rho/\rho_d)^2 = 180\,\mathrm{km}^2$, so that all stars have the same low-density equation of state. The first entry corresponds to a model with no density discontinuity.

R (km)	ρ_c (g cm^{-3})	$\sqrt{\bar{\rho}}$ (km^{-1})	ρ_d (g cm^{-3})	$\Delta\rho/\rho_d$	ν_f (kHz)	ν_p (kHz)	ν_g (kHz)
13.44	0.92×10^{15}	0.0292	–	0.0	1.666	4.045	–
12.04	1.39×10^{15}	0.0344	3×10^{14}	0.1	1.998	4.637	0.504
12.22	1.36×10^{15}	0.0337	4×10^{14}	0.1	1.962	4.548	0.567
12.42	1.32×10^{15}	0.0329	5×10^{14}	0.1	1.915	4.459	0.613
12.65	1.27×10^{15}	0.0319	6×10^{14}	0.1	1.857	4.365	0.644
12.92	1.19×10^{15}	0.0310	7×10^{14}	0.1	1.792	4.260	0.659
13.21	1.11×10^{15}	0.0300	8×10^{14}	0.1	1.723	4.146	0.658
13.43	1.02×10^{15}	0.0292	9×10^{14}	0.1	1.670	4.052	0.641
10.71	2.17×10^{15}	0.0410	4×10^{14}	0.2	2.408	5.325	0.840
10.99	2.07×10^{15}	0.0395	5×10^{14}	0.2	2.330	5.155	0.912
11.35	1.95×10^{15}	0.0376	6×10^{14}	0.2	2.226	4.970	0.961
11.83	1.77×10^{15}	0.0354	7×10^{14}	0.2	2.088	4.750	0.987
12.50	1.51×10^{15}	0.0325	8×10^{14}	0.2	1.901	4.452	0.979
13.38	1.15×10^{15}	0.0294	9×10^{14}	0.2	1.680	4.072	0.906
8.68	4.44×10^{15}	0.0562	5×10^{14}	0.3	3.216	6.683	1.211
9.13	3.95×10^{15}	0.0521	6×10^{14}	0.3	3.039	6.325	1.281
9.66	3.46×10^{15}	0.0479	7×10^{14}	0.3	2.831	5.953	1.326
10.41	2.88×10^{15}	0.0428	8×10^{14}	0.3	2.553	5.506	1.339
12.15	1.87×10^{15}	0.0340	9×10^{14}	0.3	2.002	4.632	1.251

Table 2. The equilibrium parameter and the quasi-normal mode frequencies are shown as in Table 1 for stellar models with $M = 1.4\,M_\odot$ and $\Gamma = 1.67$. The polytropic coefficient K is chosen in such a way that the star with no discontinuity ($\Delta\rho/\rho_d = 0$) and those with $\Delta\rho/\rho_d = 0.1$ have the same low-density equation of state.

R (km)	ρ_c (g cm^{-3})	$\sqrt{\bar{\rho}}$ (km^{-1})	ρ_d (g cm^{-3})	$\Delta\rho/\rho_d$	ν_f (kHz)	ν_p (kHz)	ν_g (kHz)
17.96	0.72×10^{15}	0.0189	–	0.0	1.286	2.543	–
13.38	2.14×10^{15}	0.0294	4.0×10^{14}	0.1	2.035	3.747	0.641
14.05	1.86×10^{15}	0.0273	4.5×10^{14}	0.1	1.895	3.528	0.648
14.75	1.61×10^{15}	0.0254	5.0×10^{14}	0.1	1.764	3.321	0.650
15.51	1.38×10^{15}	0.0235	5.5×10^{14}	0.1	1.633	3.311	0.646
16.39	1.15×10^{15}	0.0217	6.0×10^{14}	0.1	1.495	2.892	0.635
17.32	0.94×10^{15}	0.0199	6.5×10^{14}	0.1	1.367	2.680	0.614
17.90	0.81×10^{15}	0.0190	7.0×10^{14}	0.1	1.293	2.555	0.593

Table 3. The equilibrium parameter and the quasi-normal mode frequencies are shown for stellar models with $M = 1.4\,M_\odot$ and $\Gamma = 1.83$. The first entry is a star with no discontinuity, the other stars have a discontinuity of amplitude $\Delta\rho/\rho_d = 0.2$ and the polytropic coefficient K is chosen as in Table 2.

R (km)	ρ_c (g cm^{-3})	$\sqrt{\bar{\rho}}$ (km^{-1})	ρ_d (g cm^{-3})	$\Delta\rho/\rho_d$	ν_f (kHz)	ν_p (kHz)	ν_g (kHz)
15.17	0.82×10^{15}	0.0243	–	0.0	1.490	3.308	–
10.22	3.40×10^{15}	0.0440	4.0×10^{14}	0.2	2.736	5.361	0.932
10.51	3.16×10^{15}	0.0422	4.5×10^{14}	0.2	2.639	5.185	0.961
10.82	2.94×10^{15}	0.0404	5.0×10^{14}	0.2	2.542	5.016	0.985
11.17	2.72×10^{15}	0.0385	5.5×10^{14}	0.2	2.434	4.839	1.003
11.58	2.48×10^{15}	0.0365	6.0×10^{14}	0.2	2.314	4.648	1.014
12.07	2.22×10^{15}	0.0343	6.5×10^{14}	0.2	2.177	4.434	1.016
12.71	1.92×10^{15}	0.0317	7.0×10^{14}	0.2	2.011	4.174	1.007
13.66	1.53×10^{15}	0.0285	7.5×10^{14}	0.2	1.789	3.817	0.972
15.08	1.03×10^{15}	0.0246	8.0×10^{14}	0.2	1.507	3.338	0.874

Table 4. The equilibrium parameter and the quasi-normal mode frequencies are shown as in previous tables, for stellar models with $M = 1.4\ \mathrm{M}_\odot$, $\Gamma = 2.25$ and $\Delta\rho/\rho_\mathrm{d} = 0.3$.

R (km)	ρ_c (g cm^{-3})	$\sqrt{\bar{\rho}}$ (km^{-1})	ρ_d (g cm^{-3})	$\Delta\rho/\rho_\mathrm{d}$	ν_f (kHz)	ν_p (kHz)	ν_g (kHz)
11.32	1.22×10^{15}	0.0378	–	0.0	2.005	5.361	–
8.53	3.44×10^{15}	0.0577	6.0×10^{14}	0.3	3.095	7.329	1.171
8.71	3.34×10^{15}	0.0560	7.0×10^{14}	0.3	3.031	7.145	1.253
8.92	3.21×10^{15}	0.0540	8.0×10^{14}	0.3	2.945	6.949	1.317
9.20	3.03×10^{15}	0.0516	9.0×10^{14}	0.3	2.831	6.734	1.362
9.58	2.77×10^{15}	0.0485	1.0×10^{15}	0.3	2.673	6.473	1.395
10.14	2.41×10^{15}	0.0445	1.1×10^{15}	0.3	2.445	6.116	1.368
10.60	2.12×10^{15}	0.0417	1.15×10^{15}	0.3	2.268	5.829	1.326
11.26	1.66×10^{15}	0.0381	1.2×10^{15}	0.3	2.027	5.404	1.208

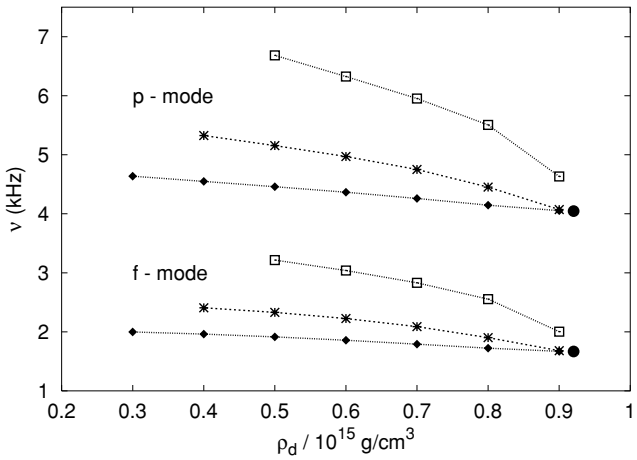

Figure 2. The f mode and the first p-mode frequencies are plotted as a function of the density at the discontinuity, ρ_d, for the models of stars with mass $M = 1.4\ \mathrm{M}_\odot$ and $\Gamma = 2$ given in Table 1. The different curves refer to assigned values of $\Delta\rho/\rho_\mathrm{d} = (0.1, 0.2, 0.3)$, increasing from bottom to top. The variation of the mode frequency with the discontinuity parameters depends on the associated variation of the mean density and the compactness of the star (see the text). All mode frequencies tend to the same limiting value (black dot) as ρ_d approaches the central density, which is the frequency of the mode when there is no discontinuity.

different values of $\Delta\rho/\rho_\mathrm{d} = (0.1, 0.2, 0.3)$. In the remaining three tables (Tables 2–4), we change the polytropic index and for each value we consider a different $\Delta\rho/\rho_\mathrm{d}$. These choices allow one to study the mode frequencies for a wide range of stellar models.

The dependence of the mode frequencies on the variables relevant to our analysis is better clarified in the following figures. In Fig. 2, we plot the frequency of the fundamental mode and of the first p mode as a function of ρ_d, for models with $\Gamma = 2$ (Table 1), and for the three selected values of $\Delta\rho/\rho_\mathrm{d}$. We choose the $\Gamma = 2$ models because they are sufficiently representative of the general behaviour. The curves representing ν_f and ν_p for different $\Delta\rho/\rho_\mathrm{d}$ tend to a limiting value (shown as a black dot in the figure), which is the frequency of the modes when there is no discontinuity inside the star, i.e. when ρ_d exceeds the central density. Both ν_f and ν_p increase with $\Delta\rho/\rho_\mathrm{d}$, and decrease with ρ_d. This behaviour is not surprising. Indeed, from the data in Tables 1–4 we see that, having fixed the mass of the NS, both the mean density and the compactness increase with $\Delta\rho/\rho_\mathrm{d}$ and decrease with ρ_d; from the Newtonian theory of stellar perturbations it is known that the f-mode frequency is proportional to $\sqrt{M/R^3}$, and the first p-mode frequency scales with the compactness of the star M/R. Thus, the results shown in Fig. 2 confirm this general behaviour, despite the structural changes produced by the density discontinuity. The dependence of ν_f and ν_p on the mean density and compactness of the star has been studied in general relativity for a large number of realistic EOSs; empirical relations have been derived between the mode frequencies and the parameters of the star, which could be used to infer the mass and the radius of neutron stars if a gravitational signal emitted by these pulsation modes were detected (Andersson & Kokkotas 1996, 1998; Kokkotas, Apostolatos & Andersson 2001). These fits were obtained on the assumption that the density is continuous inside the star, and it is interesting to see whether a discontinuity introduces deviations from the expected behaviour. For instance, in Fig. 3 we plot, as a continuous line, the linear fit that relates ν_f and $\sqrt{M/R^3}$ obtained by Andersson & Kokkotas (1998) (AK98 fit). In the same figure, we also plot the values of ν_f that we find for models with different values of Γ and $\Delta\rho/\rho_\mathrm{d}$. The frequencies of the models with $\Delta\rho/\rho_\mathrm{d} = 0$ are shown as black dots. We see that if a density discontinuity occurs in the inner core, ν_f deviates from the fit; the fit is expected to have an error of less than 1 per cent (Kokkotas et al. 2001), but the deviation introduced by a density discontinuity is certainly larger. Thus, the detection of an f-mode frequency would still allow one to estimate the mean density of the star, but with a larger uncertainty. Similar conclusions can be drawn by plotting the p-mode frequency as a function of M/R.

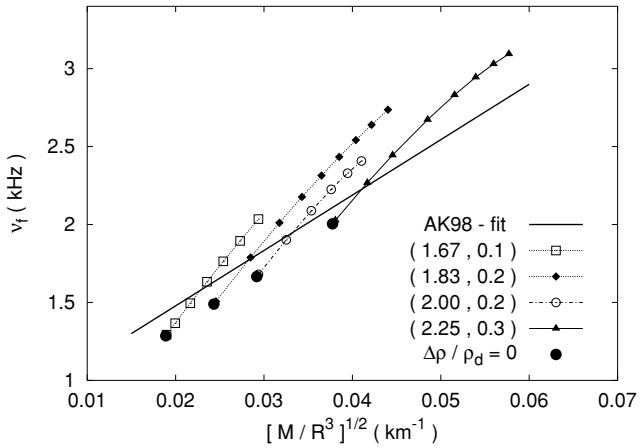

Figure 3. We show the f-mode frequency as a function of the mean density of the NS for a sample of our models, labelled with (Γ, $\Delta\rho/\rho_{\rm d}$). The fit by Andersson & Kokkotas (1998), obtained for stars without density discontinuities, is shown as a continuous line (AK98 fit), while the black dots are the f-mode frequency of our models with $\Delta\rho/\rho_{\rm d} = 0$. The figure shows that, for each assigned value of $\Delta\rho/\rho_{\rm d}$, the f-mode frequency is still a linear function of $\sqrt{M/R^3}$, as in the case of stars with no discontinuity, but with a different slope.

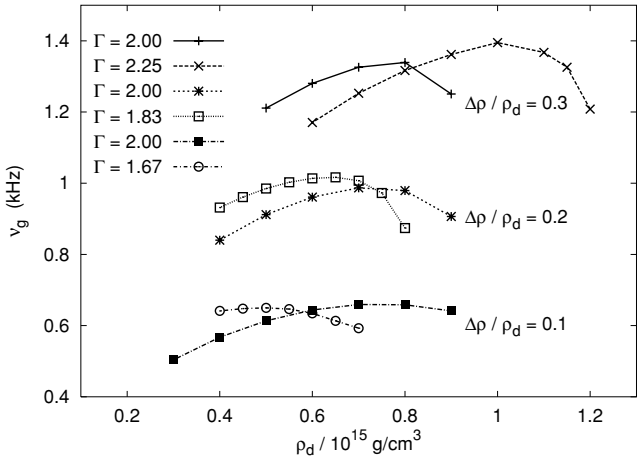

Figure 4. The g-mode frequency of the stellar models given in Tables 1–4 , is shown as a function of $\rho_{\rm d}$. It is remarkable that $\nu_{\rm g}$ depends much more on the amplitude of the density discontinuity $\Delta\rho/\rho_{\rm d}$, than on the other parameters of the EOS. Should a g mode ever be detected, this feature would allow one to infer the value of the density jump.

Let us now focus on the properties of the g mode that is produced by the density discontinuity. The possible values of $\nu_{\rm g}$ cover a wide range, $\nu_{\rm g} \approx$ [0.5–1.4] kHz (see Tables 1–4), and they are the highest-frequency g modes that one can expect in neutron stars. Indeed, g modes arising from finite-temperature effects have very low frequencies (McDermott, van Horn & Scholl 1983; McDermott, van Horn & Hansen 1988), while those arising from composition gradients in neutron star cores (Reisenegger & Goldreich 1992; Lai 1994) and to density discontinuities in the outer layers (Finn 1987; McDermott 1990) have, typically, $\nu \leqslant 200$ Hz. Thus, should a g mode be detected, one could establish whether it is caused by a discontinuity at supranuclear densities by looking at its frequency. The observation of such a g mode would also carry information on the parameters that characterize the discontinuity. This is clear from Fig. 4, where we plot $\nu_{\rm g}$ as a function of $\rho_{\rm d}$, for all the considered models. We see that the g-mode frequencies belonging to the same density jump, $\Delta\rho/\rho_{\rm d}$, cluster in a definite region of frequency, independently of the other parameters of the EOS (Γ and $\rho_{\rm d}$), and this is a remarkable feature.

Furthermore, for a fixed value of $\Delta\rho/\rho_{\rm d}$, $\nu_{\rm g}$ exhibits a maximum as a function of the location of the discontinuity. To better show this behaviour, in Fig. 5 we explicitly plot $\nu_{\rm g}$, computed for two stars with the same $\Delta\rho/\rho_{\rm d} = 0.2$ and having $\Gamma = 1.83$ and 2, respectively, as a function of the radius at which the discontinuity occurs, $R_{\rm d}$. The reason why there is such a maximum is the following. In a chemically homogeneous, zero-temperature star with no density discontinuity, the g-mode spectrum is degenerate at zero frequency. When we consider stars with $R_{\rm d}$ very close to the centre, or when we put the discontinuity very close to the surface, we are approaching the model with no discontinuity, and in both cases $\nu_{\rm g}$ tends to zero. Thus a maximum has to be expected at some $R_{\rm d}$, intermediate between these two extreme cases. For all the models we studied the maximum g-mode frequency is found when $0.4 \leqslant R_{\rm d}/R \leqslant 0.6$.

As already shown by Finn (1987) following a Newtonian analysis (Landau & Lifshitz 1959), if the discontinuity is in the low-density region near the surface of the star, the dispersion relation for the oscillation modes can be written as

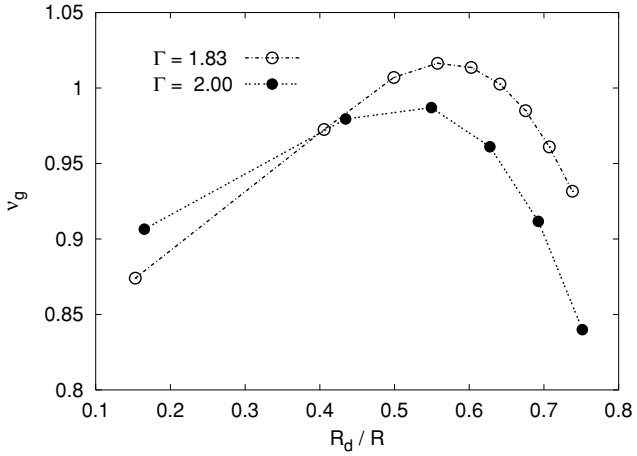

Figure 5. The discontinuity g-mode frequency is plotted as a function of the normalized radius of the internal core for two selected stellar models with $\Gamma = 1.83$ and 2, respectively. The amplitude of the density jump is $\Delta\rho/\rho_{\rm d} = 0.2$. The maximum frequency is reached when the radii of the internal core and of the outer region are comparable. For all the studied models $\nu_{\rm max}$ is reached for $0.4 \leqslant R_{\rm d}/R \leqslant 0.6$.

$$\omega_{\rm g}^2 \simeq l(l+1)\,\bar{\rho}\,\frac{\Delta\rho/\rho_{\rm d}}{1+\Delta\rho/\rho_{\rm d}}\,\frac{\Delta r}{R}, \tag{12}$$

where $\bar{\rho} = M/R^3$ is the mean density of the star, $\Delta r = R - R_{\rm d}$ and l is the order of the considered multipole. This relation is obtained by solving a stratified two-fluid problem, taking the lower-density fluid to be infinitely deep and approximating the spherical symmetry of the star by plane symmetry, assumptions that are reasonable if the density discontinuity is near the surface of the star. Obviously, they are no longer satisfied when the discontinuity occurs at high density and $R_{\rm d} \approx 0.5R$. However, we find that the maximum g-mode frequency for each assigned EOS satisfies a similar relation

$$\omega_g^{\max 2} \simeq l(l+1)\,\mathcal{C}^2\,\frac{\Delta r}{R}, \tag{13}$$

where

$$\mathcal{C}^2 \equiv \bar{\rho}_{\rm i}\,\frac{\Delta\rho/\rho_{\rm d}}{1+\Delta\rho/\rho_{\rm d}}, \tag{14}$$

which differs from the corresponding term in equation (12) only because the mean density is replaced by the mean density of the 'internal' core ($\rho > \rho_{\rm d}$), $\bar{\rho}_{\rm i}$. Considering all our stellar models, we find the following linear fit:

$$\nu_{\rm g}^{\max} = \left[0.070 + 0.905\left(\frac{\mathcal{C}}{0.025\ {\rm km}^{-1}}\right)\right]\ {\rm kHz} \tag{15}$$

with an error smaller than 2 per cent. For our models, $0.016 \leqslant \mathcal{C} \leqslant 0.037\ {\rm km}^{-1}$. This linear behaviour has an interesting consequence. Suppose that a g mode with a given frequency $\nu_{\rm obs}$ could be detected. Then, from Fig. 4 we would be able to constrain the amplitude of the density discontinuity $\Delta\rho/\rho_{\rm d}$ and from the fit (15) we could set a lower limit on $\mathcal{C}$ and consequently on $\bar{\rho}_{\rm i}$. All the EOSs with $\mathcal{C} < \mathcal{C}(\nu_{\rm obs})$ would be ruled out because they would have a g mode with a maximum frequency lower than the observed one.

4 EXCITATION MECHANISMS AND DETECTABILITY

We shall discuss three astrophysical processes that could be associated with the excitation of discontinuity g modes and to the emission of gravitational waves: the coalescence of a NS–NS binary system, the onset of a phase transition in the neutron star core and a pulsar glitch. For the last two cases, we shall estimate how much energy should be deposited into the modes in order for the emitted signal to be detectable by interferometric detectors very sensitive in the kHz frequency region.

The tidal excitation of (non-rotating) NS oscillations in binary systems has been studied extensively in the past. In the case of core g modes, it has been shown that the overlap integral between the displacement field and the tidal force field is small (Reisenegger & Goldreich 1994; Ho & Lai 1999; Lai 1994), and since the energy absorbed by a mode is proportional to the square of this integral, they are basically ineffective. To ascertain whether g modes arising from density discontinuities could be more efficiently excited in a binary system, we adopt the formalism introduced in previous works (Gualtieri et al. 2001; Pons et al. 2002a), where we computed the gravitational perturbations of a neutron star induced by an orbiting companion using a perturbative approach. We find that the typical resonance width of a discontinuity g mode ($\Delta\nu \approx 10^{-2}$ Hz) is much smaller than that of the f mode ($\Delta\nu \approx 100$–200 Hz). Similarly to what happens for the g modes arising from thermal and composition gradients, the shift that the resonant excitation of a discontinuity g mode produces in the number of cycles of the emitted signal is of the order of 10^{-2} cycles, too small to affect the detection significantly. For this reason, tidal excitation of g modes during the coalescence of NS binary systems does not seem to be an efficient mechanism for the emission of gravitational radiation, and we shall not consider it in the following.

A second excitation mechanism is the onset of a phase transition. According to current theories of stellar structure and evolution, the matter composing a neutron star may undergo a phase transition to quark matter if, at some point of the star life, a sufficiently high density is reached in its core. The critical density required to produce such a transition can be reached soon after the core collapse that gives birth to the neutron star, or at a later stage of its evolution, owing to accretion (Cheng & Dai 1998) and/or spin-down (Ma & Xie 1996). The onset of a phase transition is accompanied by a sudden reduction of the stellar radius and the difference in binding energy between the initial and final configuration is expected to be radiated away. The binding energy released during this late *mini-collapse* is of the same order as that emitted during neutron star formation following a gravitational core collapse, i.e. $\approx 2 \times 10^{53}$ erg $= 0.1\,\mathrm{M}_\odot\,c^2$ (Alcock, Farhi & Olinto 1986; Bombaci & Datta 2000). How much of this energy reservoir can be redistributed in the different modes of oscillation of the star and radiated as gravitational waves is, however, an open issue. Therefore, the only thing we can reasonably estimate is what fraction of this energy should go into the quasi-normal modes in order for the signal emitted at the corresponding frequencies to be detectable.

The quasi-normal modes of oscillation of a star may also be excited as a consequence of a glitch. Glitches are sudden changes in the rotation frequency of the neutron star crust that superimpose on the usual gradual spin-down under magnetic torque. They are observed in many pulsars and are thought to be related to quakes occurring in solid structures such as the crust, the superfluid vortices and, perhaps, the lattice of quark matter in the stellar core (Anderson & Itoh 1975; Ruderman 1976; Pines & Alpar 1985). The observed glitches are very small, with a typical fractional spin variation of approximately $\Delta\Omega/\Omega \approx 10^{-6}$–$10^{-8}$, which would be associated with an energy release of the order of $\Delta E \approx I\Omega\Delta\Omega$, where I is the moment of inertia of the star. For the glitches observed in the Crab and Vela pulsars this simple estimate gives $\Delta E \simeq 2 \times 10^{-13}\,\mathrm{M}_\odot\,c^2$ and $\Delta E \simeq 3 \times 10^{-12}\,\mathrm{M}_\odot\,c^2$, respectively. As before, we shall assume that a fraction of this energy is redistributed into the quasi-normal modes of oscillation of the perturbed star, and we shall evaluate how much is needed to excite a mode to a detectable level.

4.1 Detectability

The frequency of the discontinuity g modes we have studied are in the range $\nu_\mathrm{g} \simeq$ [0.5–1.4] kHz, while $\nu_\mathrm{f} \simeq$ [1.3–3.2] kHz and for the first p mode $\nu_\mathrm{p} \simeq$ [2.5–7.3] kHz. In order to detect a signal emitted as a consequence of the excitation of these modes a very sensitive high-frequency detector would be needed. In the following we shall consider the gravitational laser interferometric detector EURO, which has recently been proposed in a preliminary assessment study and for which the sensitivity has been estimated by Sathyaprakash and Schutz (http://www.astro.cf.ac.uk/geo/euro). EURO should be extremely sensitive in the kHz region, which is crucial for infering information concerning the interior of neutron stars from gravitational wave data, and it has been envisaged in two experimental configurations: one for which the noise curve in the frequency region 10–10^4 Hz can be written as

$$S_n(\nu) = 10^{-50}\left[\frac{3.6\times10^9}{\nu^4} + \frac{1.3\times10^5}{\nu^2} + 1.3\times10^{-3}\,\nu_k\left(1+\frac{\nu^2}{\nu_k^2}\right)\right]\mathrm{Hz}^{-1}, \tag{16}$$

where $\nu_k = 10^3$ Hz; the second configuration is the more ambitious Xylophone detector, for which the shot noise, i.e. the third term within brackets in (16), should be eliminated by running several narrow-band interferometers. We will refer to these two possible configurations as EURO and EURO–Xylo, respectively. We shall assume that the gravitation signal from a star pulsating in a quasi-normal mode is a damped sinusoid of the form (Echeverria 1989)

$$h(t) = \mathcal{A}\mathrm{e}^{(t_\mathrm{arr}-t)/\tau}\sin\left[2\pi\nu\,(t-t_\mathrm{arr})\right], \tag{17}$$

where t_arr is the arrival time and τ is the damping time of the oscillation. The amplitude $\mathcal{A}$ can be expressed in terms of the total energy $\Delta\mathrm{E}_\odot = \Delta E/\mathrm{M}_\odot\,c^2$ deposited into the mode, and of the distance D of the source by (Kokkotas et al. 2001)

$$\mathcal{A} \simeq 7.6\times10^{-23}\sqrt{\frac{\Delta\mathrm{E}_\odot}{10^{-10}}\,\frac{1\mathrm{s}}{\tau}}\left(\frac{1\,\mathrm{kpc}}{D}\right)\left(\frac{10^3\,\mathrm{Hz}}{\nu}\right). \tag{18}$$

Given a detector with noise spectrum $S_n(\nu)$, and assuming that the matched filtering technique is used to extract the signal, the signal-to-noise (S/N) ratio, can be written as

$$\mathrm{S/N} = \left[\mathcal{F}\,\frac{\mathcal{A}^2\tau}{2S_n}\right]^{1/2}, \tag{19}$$

where $\mathcal{F} = 4Q^2/(1+4Q^2)$ is a form factor and $Q = \pi\nu\tau$ is the quality factor of the oscillation.

It should be noted that in the case of discontinuity g modes, since the gravitational damping time is in the range $\tau \approx (10^7$–$10^{12})$ s, the oscillations will be damped by other dominant dissipative mechanisms rather than by the emission of gravitational waves. In newly born neutron stars (or hybrid stars with a quark core) the dominant damping mechanism is neutrino viscosity, with a typical time-scale of 10–10^2 s (van den Horn & van Weert 1981; Goodwin & Pethick 1982; Thompson & Duncan 1993). In the glitches scenario (or other similar excitations occurring in late stages of the evolution of neutron stars) the neutron star is cold and neutrinos are not coupled to the matter. The dissipative mechanisms are then associated with the kinematical properties of matter. In this case, bulk, shear viscosity and boundary layer dissipation are more efficient than gravitational damping. In any case, the typical dissipative time-scales are thought to be much larger than the neutrino damping time-scale in protoneutron (quark) stars (Bildsten & Ushomirsky 2000), but a word of caution is needed. It has been found that quark-matter viscosity is much larger than that of normal neutron star matter (Madsen 1992), and therefore it would quickly damp

Table 5. The amount of energy that should be radiated in gravitational waves at the frequency of a given mode, in order for the signal to be detectable with S/N = 3 by the EURO detector configurations. The source distance is taken to be $D = 15$ Mpc and 10 kpc (see the discussion in the text).

Mode	$\nu_{\rm mode}$	$D = 15$ Mpc		$D = 10$ kpc	
		ΔE (Euro)	ΔE (Euro–Xylo)	ΔE (Euro)	ΔE (Euro–Xylo)
$g_{\rm core}$	0.1 kHz	$3.5 \times 10^{-7}\ {\rm M}_\odot\ c^2$	$3.4 \times 10^{-7}\ {\rm M}_\odot\ c^2$	$1.6 \times 10^{-13}\ {\rm M}_\odot\ c^2$	$1.5 \times 10^{-13}\ {\rm M}_\odot\ c^2$
$g_{\rm disc}$	0.5 kHz	$3.9 \times 10^{-7}\ {\rm M}_\odot\ c^2$	$1.0 \times 10^{-7}\ {\rm M}_\odot\ c^2$	$1.7 \times 10^{-13}\ {\rm M}_\odot\ c^2$	$4.5 \times 10^{-14}\ {\rm M}_\odot\ c^2$
	1.4 kHz	$5.4 \times 10^{-6}\ {\rm M}_\odot\ c^2$	$9.2 \times 10^{-8}\ {\rm M}_\odot\ c^2$	$2.4 \times 10^{-12}\ {\rm M}_\odot\ c^2$	$4.1 \times 10^{-14}\ {\rm M}_\odot\ c^2$
f	2.3 kHz	$3.0 \times 10^{-5}\ {\rm M}_\odot\ c^2$	$9.2 \times 10^{-8}\ {\rm M}_\odot\ c^2$	$1.4 \times 10^{-11}\ {\rm M}_\odot\ c^2$	$4.1 \times 10^{-14}\ {\rm M}_\odot\ c^2$
p_1	5.5 kHz	$8.7 \times 10^{-4}\ {\rm M}_\odot\ c^2$	$9.1 \times 10^{-8}\ {\rm M}_\odot\ c^2$	$3.8 \times 10^{-10}\ {\rm M}_\odot\ c^2$	$4.0 \times 10^{-14}\ {\rm M}_\odot\ c^2$

the oscillations in the dense quark core ($\tau \sim 10^{-2}$ s). However, these results are still under debate, and it remains to be carefully analysed how the outer shell would react to the strong damping in the inner region, and whether or not boundary effects would change the picture. Note, however, that, for the range of frequencies considered in this paper, the quality factor $Q \gg 1$ as long as τ is greater that, say, 10^{-2} s; thus, the form factor in equation (19) can be taken as being equal to one, and the signal-to-noise ratio happens to be quite insensitive to the damping time.

In the following, we shall estimate the amount of energy that should go into a quasi-normal mode to produce a gravitational signal detectable with a signal-to-noise ratio of S/N = 3, either by EURO or by the EURO–Xylo detector. For g-mode pulsations, we consider the two limiting frequencies $\nu_1 = 0.5$ kHz and $\nu_2 = 1.4$ kHz, being the g-mode frequency of all our models included in this range. The excitation of a core g mode at 0.1 kHz (Reisenegger & Goldreich 1992; Lai 1994) is also computed for comparison. For the f- and p modes, our estimates are made for two frequencies, $\nu_{\rm f} = 2.3$ kHz and $\nu_{\rm p} = 5.5$ kHz, which are obtained as an average over the corresponding range of variation for all our models. The gravitational damping time of the fundamental and p mode are smaller than the other dissipative time-scales; thus, in this case the emission of gravitational waves is the dominant dissipative mechanism and both $\tau_{\rm f}$ and $\tau_{\rm p}$ have been used explicitly in our estimates.

For the two different excitation scenarios, mini-collapse and glitches, we shall consider sources located at distances $D = 15$ Mpc and 10 kpc, respectively. Note that the Virgo cluster, with its some 2×10^3 members, is at $D \approx 15$ Mpc and that the Vela and Crab pulsars, which are known to produce glitches, are at distances of $D = 0.5$ and 2 kpc, respectively.

Our estimates are given in Table 5, and show that the high-frequency detectors would be a very interesting instrument to probe, through gravitational signals, the nature of neutron stars interiors. Note that, since for the EURO configuration the sensitivity at high frequency is strongly limited by the shot noise, a p mode at $\nu_{\rm p} = 5.5$ kHz could be detected only with the advanced EURO–Xylo configuration. If one focuses on the fundamental mode and the discontinuity g mode, the minimal energies required to detect a signal with S/N = 3 with the EURO detector range within $1.6 \times 10^{-13} \leqslant \Delta E\ /{\rm M}_\odot\ c^2 \leqslant 3.0 \times 10^{-5}$, depending on the source distance and on the frequency of the signal. With the EURO–Xylo configuration, this range becomes $4.1 \times 10^{-14} \leqslant \Delta E\ /{\rm M}_\odot\ c^2 \leqslant 3.4 \times 10^{-7}$. As mentioned before, the amount of binding energy that is expected to be released in a mini-collapse is approximately the same as that emitted during a core-collapse supernova. In the supernova case, it has been suggested that the fraction of this energy radiated in gravitational waves is in the range $[10^{-8}$–$10^{-6}]\ {\rm M}_\odot\ c^2$ (Mönchmeyer et al. 1991; Dimmelmeier, Font & Müller 2001; Zwerger & Müller 1997); if we assume that a comparable amount of energy also goes in gravitational waves in the case of a mini-collapse, the chance for a quasi-normal mode signal to be detectable from a source closer than 15 Mpc is promising. The situation is clearly even more interesting for Galactic sources, since the amount of energy required to excite a mode at a detectable level is typically a small fraction of the total energy reservoir.

5 CONCLUSIONS

According to the relativistic theory of stellar perturbations, a star perturbed by any external or internal process emits gravitational waves at the characteristic frequencies of its quasi-normal modes. It has been shown that both the mass and the radius of a pulsating cold neutron star could be inferred, if the quasi-normal modes were identified by a spectral analysis in the detected wave (Andersson & Kokkotas 1998). More recently, the possibility of tracing the presence of a superfluid core through the detection of superfluid modes has also been investigated (Lee 1995; Andersson & Comer 2001). As described in the introduction, g modes are also good markers of the internal composition of a neutron star: low-frequency g modes indicate a non-homogeneous composition in the outer layers or in the core of the star, or a thermal profile, whereas the high-frequency g modes that we study in this paper, are associated with phase transitions occurring at supranuclear densities (Sotani et al. 2001). Although the analysis has been restricted to simplified polytropic EOSs, our results can be generalized to realistic equations of state, since it is known that the oscillation frequencies depend more on global properties, such as mass and radius, than on the specific form of the microscopic interactions. We have analysed models of stars with a mass of 1.4 $\rm M_\odot$, since astrophysical observations show that most of the well-measured masses of neutron stars in binary systems cluster in a narrow range around this value.

We find that high-frequency discontinuity g modes exhibit several interesting features: (i) the linear relation known to exist between the frequency of the fundamental mode and the square root of the average density, still holds for neutron stars with density discontinuities. Thus, a measure of the f-mode frequency would be useful to constrain the neutron star radius, provided the mass is measured independently, even when a phase transition takes place in its core. However, the presence of the discontinuity introduces a larger error on the NS radius determination.

(ii) Should density discontinuities actually exist, the associated g mode will have a frequency of approximately 1 kHz, somewhat lower than that of the f mode, and therefore clearly distinguishable. It may be worth noting that thermal or chemical g modes appear at significantly lower frequencies (<200 Hz). (iii) Since the g-mode frequency strongly depends on the amplitude of the discontinuity, it could be used to infer the value of $\Delta\rho/\rho_{\rm d}$. In addition, since the maximum of $\nu_{\rm g}$, considered as a function of the discontinuity radius $R_{\rm d}$, is related to $\Delta\rho/\rho_{\rm d}$ and to the average density, $\bar{\rho}_{\rm i}$, of the core internal to $R_{\rm d}$ (see equations 14 and 15) it would be possible to set a lower bound on $\bar{\rho}_{\rm i}$ and to rule out all EOSs for which the combination $\mathcal{C}^2 \equiv \bar{\rho}_{\rm i}\,\frac{\Delta\rho/\rho_{\rm d}}{1+\Delta\rho/\rho_{\rm d}}$ is smaller than the observed one.

In the spirit of previous works (Andersson & Comer 2001), which discussed the observability of oscillation modes produced by the existence of superfluid components in the interior of a neutron star, we have analysed some astrophysical processes in which high-frequency modes could be excited, and we have evaluated the amount of energy that the modes should convey to produce a gravitational signal detectable with $S/N = 3$ by the high-frequency gravitational detectors under study. We find that the required energy does not conflict with the estimates of the energy expected to be released in gravitational waves at the onset of a phase transition, or during a glitch. In particular, the detector EURO, especially in the configuration known as EURO–Xylophone, would have a significant chance to reveal the gravitational signal associated with the excitation of the fundamental mode, of the first pressure mode and of the discontinuity g mode following a Galactic glitch or a stellar core collapse or a mini-collapse induced by the onset of a phase transition to quark matter within 10–15 Mpc. By cross-correlating the information carried by these mode frequencies, and in particular by the high-frequency discontinuity g modes, we would acquire extremely valuable indications on the properties of nuclear matter at supranuclear density.

ACKNOWLEDGMENTS

We thank O. Benhar for useful discussions. We thank B.S. Sathyaprakash for providing us with the power spectral density of the EURO detector. This work has been supported by the EU Programme 'Improving the Human Research Potential and the Socio-Economic Knowledge Base' (Research Training Network Contract HPRN-CT-2000-00137). JAP is supported by Marie Curie Fellowship no HPMF-CT-2001-01217.

REFERENCES

Alcock C., Farhi E., Olinto A., 1986, ApJ, 310, 261
Alford M.G., Rajagopal K., Reddy S., Wilczek F., 2001, Phys. Rev. D, 64, 074017
Anderson P.W., Itoh N., 1975, Nat, 256, 25
Andersson N., Comer G.L., 2001, Phys. Rev. Lett., 24, 241101
Andersson N., Kokkotas K.D., 1996, Phys. Rev. Lett., 77, 4134
Andersson N., Kokkotas K.D., 1998, MNRAS, 299, 1059
Bildsten L., Ushomirsky G., 2000, ApJ, 529, L33
Bombaci I., Datta B., 2000, ApJ, 530, L69
Chandrasekhar S., Ferrari V., 1990, Proc. R. Soc. Lond. A, 432, 247
Chandrasekhar S., Ferrari V., Winston R., 1991, Proc. R. Soc. Lond. A, 434, 635
Cheng K.S., Dai Z.G., 1998, ApJ, 492, 281
Detweiler S., Lindblom I., 1985, ApJ, 292, 12
Dimmelmeier H., Font J.A., Müller E., 2001, ApJ, 560, L163
Echeverria F., 1989, Phys. Rev. D, 40, 3194
Finn L.S., 1986, MNRAS, 222, 393
Finn L.S., 1987, MNRAS, 227, 265
Glendenning N.K., 1992, Phys. Rev. D, 46, 1274
Goodwin B.T., Pethick C.J., 1982, ApJ, 253, 816
Gualtieri L., Berti E., Pons J.A., Miniutti G., Ferrari V., 2001, Phys. Rev. D, 64, 104007
Heiselberg H., Hjorth-Jensen M., 2000, Phys. Rep., 328, 237
Ho W.C.G., Lai D., 1999, MNRAS, 308, 153
Kokkotas K.D., Apostolatos T., Andersson N., 2001, MNRAS, 320, 307
Lai D., 1994, MNRAS, 270, 611
Landau L., Lifshitz E., 1959, Fluid Mechanics. London, Pergamon
Lee U., 1995, A&A, 303, 515
Lindblom I., Detweiler S., 1983, ApJ Suppl. Ser., 53, 73
Ma F., Xie B., 1996, ApJ, 462, L63
Madsen J., 1992, Phys. Rev. D, 46, 3290
McDermott P.N., 1990, MNRAS, 245, 508
McDermott P.N., van Horn H.M., Scholl J.F., 1983, ApJ, 268, 837
McDermott P.N., van Horn H.M., Hansen C.J., 1988, ApJ, 325, 725
Mönchmeyer R., Schäfer G., Müller E., Kates R., 1991, A&A, 246, 417
Osherovich V., Titarchuk L., 1999, ApJ, 522, L113
Pines D., Alpar M.A., 1985, Nat, 316, 27
Pons J.A., Reddy S., Prakash M., Lattimer J.M., Miralles J.A., 1999, ApJ, 513, 780
Pons J.A., Steiner A.W., Prakash M., Lattimer J.M., 2001, Phys. Rev. Lett., 86, 5223
Pons J.A., Berti E., Gualtieri L., Miniutti G., Ferrari V., 2002a, Phys. Rev. D, 65, 104021
Pons J.A., Walter F.W., Lattimer J.M., Prakash M., Neuhäuser R., An P., 2002b, ApJ, 564, 981
Prakash M., Bombaci I., Prakash M., Ellis P.J., Lattimer J.M., Knoren R., 1997, Phys. Rep., 280, 1

Reisenegger A., Goldreich P., 1992, ApJ, 395, 240
Reisenegger A., Goldreich P., 1994, ApJ, 426, 688
Ruderman M., 1976, Nat, 203, 213
Rutledge R.E., Bildsten L., Brown E.F., Pavlov G.G., Zavlin V.E., 2001, ApJ, 559, 1054
Sotani H., Tominaga K., Maeda K., 2001, Phys. Rev. D, 65, 024010
Stella L., Vietri M., 1999, Phys. Rev. Lett., 82, 17
Strohmayer T.E., 1993, ApJ, 417, 273
Thompson C., Duncan R., 1993, ApJ, 408, 194
Thorsett S.E., Chakrabarty D., 1999, ApJ, 512, 288
van den Horn L.J., van Weert Ch. G., 1981, ApJ, 251, L97
Zwerger T., Müller E., 1997, A&A, 320, 209

This paper has been typeset from a TEX/LATEX file prepared by the author.